Kufa Journal of Engineering
Vol. 16, No. 4, October 2025, P.P. 419-434
Article history: Received 16 January 2025, last revised 22 February 2025, accepted 26 February 2025

STUDYING THE TOUGHNESS, STIFFNESS AND DUCTILITY INDEX OF CONCRETE SLAB RESTED ON WINKLER FOUNDATION REINFORCED WITH DIFFERENT SYNTHETIC TYPES OF FIBER MESHES

Mohammed Ali Basheer[1,*] and Sofyan Y. Ahmed[2]

[1] MSc student/University of Mosul, college of engineering, Civil Dept, Email:mohammed.23enp41@student.uomosul.edu.iq.

[2] Assi. Prof. PhD. /University of Mosul / college of engineering - Civil Dept, Email:Sofyan1975@uomosul.edu.iq.

[*] Corresponding Author.

https://doi.org/10.30572/2018/KJE/160424

ABSTRACT

Concrete slabs of (800×800)mm and a thickness of)100(mm resting on Winkler support, for subgrade reaction of (0.028)N/mm^3, and strengthened with different types of synthetic fiber meshes, that are fiberglass, polypropylene, carbon, geogrid, and waste rubber, are used to study the characteristics of toughness, stiffness and ductility index of these slabs incorporated with these meshes. The addition of these fibers increases the rigidity of slabs resting on the ground, to reduce the damage as minimum as possible, which keeps pace with the current development of using these materials. The experimental results show that the toughness and stiffness have been significantly improved in all the specimens strengthened with these meshes, especially for the specimens for carbon fiber mesh, where the increase was 187.0% and 33.7% respectively. The lowest increase percent in toughness of 12.9% in the case of strengthening by waste rubber, and the lowest increase percent in stiffness of 8.1% in the case of strengthening by polypropylene mesh While the specimen reinforced with geogrid showed a weakness in the ductility index (2.0), compared to the highest value for the models reinforced with carbon fibers of (3.3).

KEYWORDS

Ductility, Toughness and Stiffness.

1. INTRODUCTION

One of the most our everyday lives used materials is reinforced concrete because of its incredible qualities, such as compressive strength (Baarimah and Syed Mohsin, 2017). Helps to provide the slab stiffness and distribute loads uniformly throughout it. It's strengthened by the use of reinforcing steel to enhance its resistance to applied loads and stresses brought on by tension applied to it (Shi et al., 2023). The ACI Code states that concrete floor slabs are essential structural components of built structures where they are used for a variety of purposes including highways, walkways, and industrial slabs (ACI, 2006). However, concrete lacks resistance when subjected to different stresses, so the use of fibers was invented to improve the mechanical properties of concrete (Journal, 2010). Glass, steel, polypropylene, and other materials can be used to create fibers, which are tiny, thin, thread-like reinforcing materials that are flexible under pressure (Ischenko and Borisova, 2020). These fibers (glass, polypropylene, carbon, geogrid, waste rubber) most of these fibers have similar properties to each other, as when added to concrete they greatly reduce the growth of concrete cracks and increase the tensile strength, durability, and flexibility of concrete (Jaber, Mohammed and Abbas, 2021). Moreover, there are special properties for some fibers, such as, glass fibers (GL) are suitable for use in industrial and marine environments due to their flexibility towards salts and acids (Milind V. Mohod, 2015),(Kamonna and Al-sada, 2021). Polypropylene fibers (PP) are characterized by their non-reaction to water and do not absorb concrete water, which increases the material's resistance to shocks and corrosion (Suksawang, Mirmiran and Yohannes, 2014). Carbon fiber (CR) is used in high-performance applications, including automotive and aircraft parts, and has very high tensile strength (Abbas and Al-Zuhairi, 2022). Geogrid fiber (GG)greatly reduces deformation and enhances the mechanical properties of concrete including foundation reinforcement, and leveling of soil slopes (Koerner, 2005). Waste Rubber fiber (WR) has high resistance to shock and vibration (Etefa and Mosisa, 2020). The dimensions of the slab were chosen based on the work being done in a laboratory, and it is not possible to perform them on large samples that represent reality, as the selection of those dimensions was based on a literature review (Tahwia et al., 2024), which is a close representation of reality so that the dimensions are proportional to the thickness.

Sorelli et al., (2006) investigated the behavior of reinforced concrete slabs experimentally using steel fibers of various diameters and shapes. The findings show that steel fibers greatly improve the ductility and flexibility of slabs, raise the load-bearing capacity of concrete, and drastically lower the likelihood of concrete breaking (Sorelli, Meda and Plizzari, 2006). Sucharda et al., (2017) Steel fibers advantages in concrete slabs were investigated, with an emphasis on the material characteristics and how the fiber's affected the concrete strength. The findings demonstrated that the tensile and flexural strengths were significantly impacted by the fibers (Sucharda et al., 2017). Tahwia et al.,(2024) also investigated the experimental investigation of rubberized concrete slab-on-grade using five models of reinforced concrete slabs, measuring (1000×1000) mm and (60) mm thick, The findings demonstrated that concrete slabs with crumbly rubber had a higher durability than the control slab. And shown good resilience to lower the propagation of cracks (Tahwia et al., 2024).

In the present study, six concrete slab specimens (800×800×100) mm of reinforced with (BRC) mesh (Ø4mm@150mm) are used; one of the slabs serves as a control, and the other five specimens are reinforced with various fiber meshes (glass, polypropylene, carbon, geogrid, and waste rubber) and rest on the ground, which is represented in a Winkler model made up of (12) rubber supports resting on an (800×800) mm steel plate base with a (10) mm thickness to give the value of subgrade reaction (kw) which is to simulate the soil during the testing. The present study research aims to compare the fiber mesh-reinforced slabs with the reference slab and to investigate the toughness, stiffness, ductility, and load-carrying capacity of each specimen, following the crack pattern and yielding with loads of each type are the main variables.

2. EXPERIMENTAL APPROACH

2.1. Materials

2.1.1. Cement

All experimental materials were cast using regular Ordinary Portland Cement (OPC) of the Sinjar cement type, and they underwent chemical and physical testing, and results as shown in Table 1 and 2 respectively. The outcomes satisfied Iraqi Specification No. 5/2019 requirements and criteria.

Table 1: Chemical Properties of Cement

Chemical Compounds	Content (%)	Limits of Iraqi Specifications No.5 (2019)
SO_3	1.92	≤ 2.5% if C_3A≤ 5% ≤2.8% if C_3A≤ 5%
C_2S	26.67	—
C_3S	45.60	≤ 3.5
C_3A	6.04	—

Table 2: Physical Properties of Cement

Properties	Results	Limits of Iraqi Specifications No.5 (2019)
Initial Setting Time (minutes)	120	≥ 45 min
Final Setting Time (hrs.)	195	≤600 min
2 days Compressive Strength (MPa)	23.2	≥10
28 days Compressive Strength (MPa)	43.2	≥42.5
Fineness for Sieve No. 170 (%)	2.6	≤10
Soundness by Le Châtelet (mm)	2.3	≤10

2.1.2. Fine aggregate

Natural river sand with a maximum size of (4.75) mm. The physical properties and sieving analysis were carried out in the Concrete Technology Laboratory, University of Mosul as shown in Tables 3 and 4. Iraqi Regulation No. 45 of 1984.

Table 3: Physical Properties of fine aggregates

Physical Properties	Test Result	Iraqi Specifications No.5 (1984)
Sulfate Content (%)	0.11	≤0.5
Absorption (%)	1.80	—
Specific Gravity	2.58	—
Bulk density (kg/m³)	1550	—

Table 4: Fine aggregate properties

Sieve Size (mm)	Passing (%)	Iraqi Specifications No.45 (1984)
4.75	96.5	90-100
2.36	80.0	75-100
1.18	65.5	55-90
0.6	54.3	35-59
0.3	28.9	8-30
0.15	4.7	0-10

2.1.3. Coarse aggregate

The experimental samples were cast using gravels no larger than (12.5) mm, and the Concrete Technology Laboratory, College of Engineering, University of Mosul, conducted the screening analysis and physical testing. As shown in Tables 5 and 6 respectively.

Table 5: Coarse aggregate properties

Sieve Size (mm)	Passing (%)	Iraqi Specifications No.45 (1984)
19	100	100
12.5	94	100-90
9.5	59	70-40
4.75	1	15-0
2.36	0	5-0

Table 6: Physical Properties of coarse aggregates

Physical Properties	Test Result	Iraqi Specifications No.5 (1984)
Sulfate Content, %	0.031	≤ 0.1
Porosity %	2.20	—
Specific Gravity	2.61	—
Bulk density (kg/m³)	1620	—

2.1.4. Water

Use regular drinking water to mix all the ingredients that go into the concrete mixture.

2.1.5. Reinforcing steel

Using BRC reinforcement (Ø4mm@150mm) in the concrete slab with overall dimensions of (780×780) mm at a distance of (55) mm from the base of the wooden form. This reinforcement done for was all specimens, as shown in Fig. 1a. The test of steel mesh is performance according to ASTM A615-16 (ASTM A615/A615M 16, 2016). As shown in Table 7.

Table 7: Properties of reinforcing steel bars

Item	Test result
Actual Diameter (mm)	4
Yield Stress (MPa)	562
Ultimate Strength (MPa)	670
Total Elongation (%)	9

2.1.6. Fiber meshes (glass, polypropylene, carbon, geogrid, waste rubber)

Fiber meshes (glass and carbon plastic) with equivalent areas were used after calculating the cross-sectional area of each fiber as shown in Table 8 as strengthening for reinforced concrete. The test with the fiber meshes was conducted in the Testing Materials Laboratory at the University of Mosul / College of Engineering, and the results are shown in Fig.2. Fiber meshes were used to strengthen the concrete slab in the tension zone at a distance of (25) mm from the base of the wooden form as shown in Fig.1. The equivalent area of (4) mm^2 for synthetic fiber meshes was chosen according to the sections available in the local markets.

Table 8: Area of fiber section and equivalent area of each mesh per (50 mm length)

Fiber mesh	Area of fiber section (mm^2)	Area of 1-mesh per (50 mm length)	Equivalent area (mm^2)
Glass	0.175	1.94	3.88 (2 meshes)
Plastic	0.66	1.99	3.96 (2 meshes)
Carbon	1.0	8.0	4.00 (0.5 mesh)
Geogrid	2.0	4.0	4.00 (1 mesh)
Waste rubber	2.0	4.0	4.00 (1 mesh)

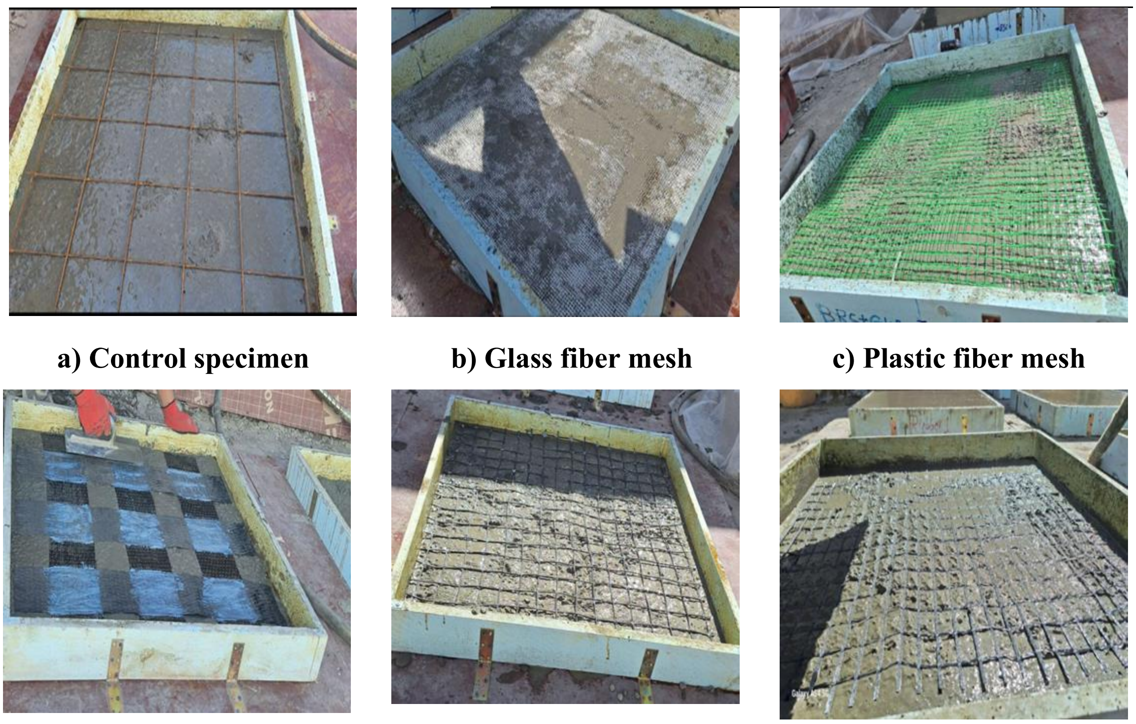

a) Control specimen **b) Glass fiber mesh** **c) Plastic fiber mesh**

d) Carbon fiber mesh **e) Geogrid fiber mesh** **f) Waste rubber fiber mesh**

Fig. 1. Experimental specimens with fiber meshes

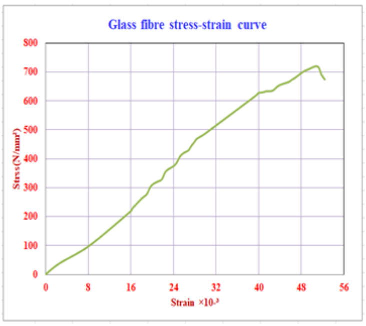

a) Glass fiber stress-strain curve

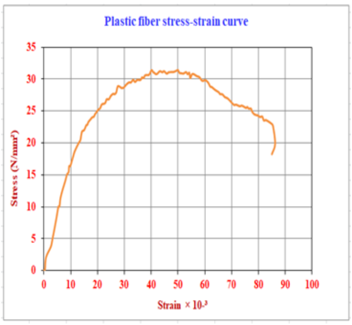

b) Plastic fiber stress-strain curve

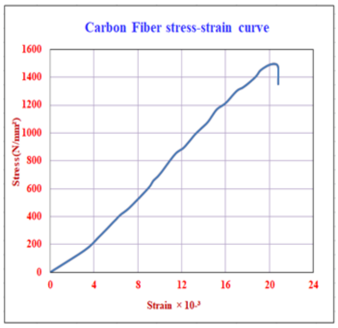

c) Carbon fiber stress-strain curve

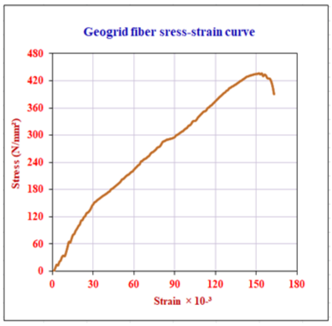

d) Geogrid fiber stress-strain curve

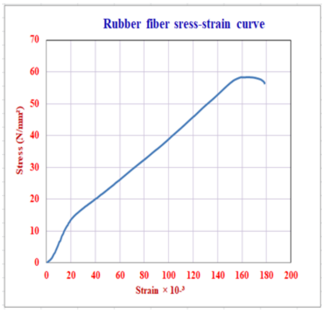

e) Waste rubber fiber stress-strain curve

Fig. 2. The stress-strain behavior of different fibers in tensile test

2.2. Concrete Mixture

The mixture used in the research of design compressive strength f_{cu}=30 MPa, the gradients of this mixture are displayed in Table 9.

Table 9: Concrete design mix characteristics.

Description	Results
Design compressive strength (MPs)	30
Cement content (kg/m^3)	380
Fine aggregate content (kg/m^3)	800
Coarse aggregate content (kg/m^3)	950
Tap water content (kg/m^3)	175

2.3. Preparation of Winkler support and testing setup

The slab resting on the ground with form dimensions of (800×800) mm and a thickness of (100) mm is shown in Fig. 3. After casting the samples and reinforcing them with different fiber meshes, the slab is placed upon examination on a steel base containing (12) rubber supports, as shown in detail in Fig. 5b, to simulate the soil. The specimens are examined using the examination device shown in Fig.6b. The details of the reinforcement and its location, the location of the load in the center of the specimen, and the dimensions of the rubber supports are shown in the side view of the sample upon examination as in Fig. 6a. The locations of the Linear Variable Differential Transformer (LVDT) in the sample to monitor deformations in the center and sides are shown in Fig. 5a, where they are connected to the data logger reader shown in Fig. 4.

2.4. Mechanical properties of slab concrete

Table 10 Shows the values of the mechanical properties, which consist of (compressive strength, elastic modulus, splitting strength, and flexural strength) at 28 days.

Table 10: Mechanical properties of concrete

Item	Sample	Test result
Compressive strength (MPa)	Cubic (150×150×150) mm	32.4
Elastic modulus (MPa)	Cylinder (Ø150×300) mm	28500
Splitting strength (MPa)	Cylinder ((Ø150×300) mm	2.3
Flexural strength (MPa)	Prism (500×100×100) mm	3.3

Fig. 4. Data logger used for control the loading and measuring the deflection in slab.

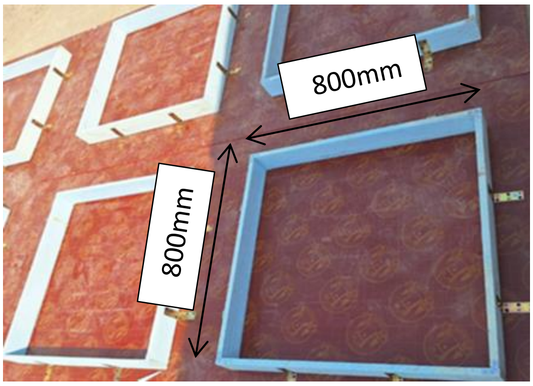

Fig. 3. Experimental specimen form

2.5. Subgrade reaction calculations

To reproduce a Winkler foundation, (12) rubber supports were placed under the slab as shown in Fig. 5b. These supports are fixed on a square steel plate having dimensions of testing (800×800) mm and a thickness of (10) mm. These rubber supports provide a good approximation of a continuous Winkler soil. The rubber stiffness was determined by compression tests performed on each piece, with an average result of (7.5) kN/mm. By considering the influence area of each rubber piece (50×50) mm, the Winkler constant (k_w) was of (0.028) N/mm^3, which corresponds to a uniformly graded dense sandy soil according to ACI classification.

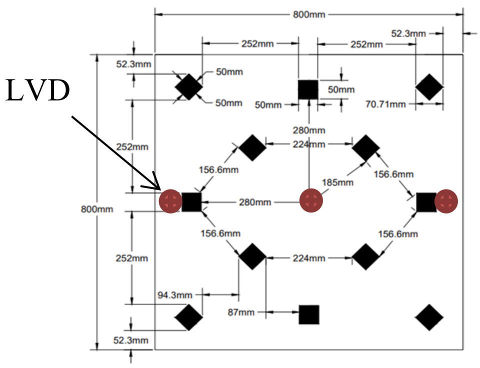

a) Arrangement of Winkler supports and LVDT location

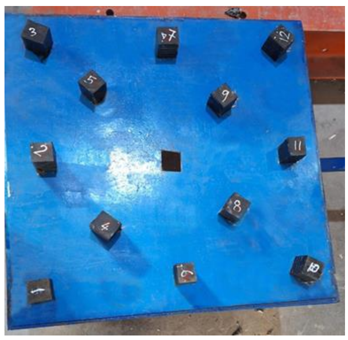

b) Winkler support model

Fig. 5 Winkler supports, Geometry and model

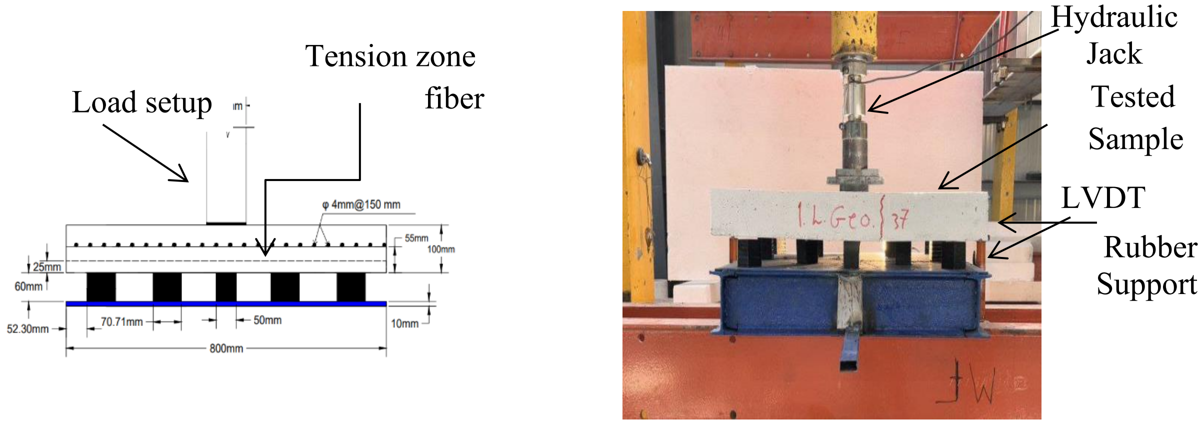

a) Cross-section details of reinforcing slab resting on a Winkler support **b) Experimental test setup**

Fig. 6. Test setup and cross section details of slab on ground

3. TEST RESULTS AND DISCUSSIONS

Six concrete slabs strengthened with different types of fiber mesh were tested by applying a load to the center. The load was gradually increased until failure. To further understand the structural behavior of the slabs, the data are discussed using five categories, failure modes and crack pattern, load-deflection behavior, first cracking and ultimate load, ductility index, and stiffness.

3.1. Failure modes and crack pattern.

Fig.7 shows the cracking and fracture patterns of the prepared slabs (BRC, GL, PP, CR, GG, and WR). After applying axial load to the experimental specimens, each specimen failed to develop a fracture in the middle of the slab. This failure was confirmed when the load was observed to drop rapidly from the slab after the first crack appeared as the fiber meshes began to rupture. As the load increased and grew again, the first crack developed on the tension side of the slab and the steel within the concrete began to resist the load. As the load increased, more cracks appeared and the number of cracks increased and they spread linearly from the center of the slab to the margins and edges of the concrete slab. Circumferential cracks began to appear around the slab. In addition, large cracks were formed at an angle of approximately 38-45 degrees. The fiber mesh strengthened concrete slabs had higher load-bearing capacity and less crack development than the reference slab, and the fiber meshes improved the ductility of the slab on the Winkler foundation, delayed the failure of the slabs, and avoided sudden failure (Tahwia et al., 2024),(Roesler et al, 2006). It was also found that the geogrid strengthen slab has more cracks but is not as large as the other slabs as shown in Fig.8e. The carbon fiber mesh has a great effect on reducing cracking and increasing the strength of concrete due to the high tensile strength of carbon fiber. Shi (Shi et al., 2023) and Tahwia (Tahwia et al., 2024) examined the slab at the ground under static loads, and their findings are in line with our findings.

3.2. Load–deflection behavior

The load-deflection curve in Fig. 8 supports the observed response of concrete slabs (BRC, GL, PP, CR, GG, and WR) under a central load. The slabs reach their maximum load before suddenly losing their load-bearing capacity and failing to fracture, indicating a decrease in strength and ductility. These curves are consistent with previous research (Nimnim and Fakhri, 2022),(Aljebory and Kamonna, 2025). The deflection at the center of the concrete slab as shown in Fig. 5a was measured by the sensor at each load increment throughout the test procedure. During the incremental loading process, several distinct stages are observed in the elastic region. The deflection increases significantly at a constant rate. Then as cracks begin to form and propagate, the deflection rate accelerates, leading to a faster increase. This trend continues until the tensile stress of the reinforcing steel reaches the yield point. At this point, the slope of the deflection curve decreases. Finally, the test is terminated when the deflection continues to increase without any simultaneous increase in the applied load. The load-deflection curves are in three stages. The first stage (the non-cracked stage) has almost linear load-deflection curves. The second stage, sometimes referred to as the pre-yield stage, occurs between the cracking load and the yield load. As shown in Fig. 8, flexural cracks appear on the slab tensile side at this point, and the mesh fiber material begins to rupture, all samples passed this stage. The last step is sometimes referred to as the post-yield stage. The load starts to drop as the specimen's deflection and crack openings increase after it has reached its maximum bearing strength. Eventually, the specimen approaches ultimate failure and collapses entirely. The slope of the curve was significantly affected by the content and presence of fiber meshes. The highest improvement in ductility was in the carbon fiber mesh strengthen specimen compared to the reference specimen. To compare the behavior between all fiber meshes in terms of response, Fig.9 shows differences between the response of these tiles, in which the highest response is for the slab strengthened with carbon fibers and the lowest response is for the slab strengthened with polypropylene fiber, noting that the deviation was the highest in the slab strengthened with carbon fiber, while the lowest deflection was in the slab strengthened with waste rubber fiber.

3.3. First cracking and ultimate load

Each specimen was examined until the first crack appeared as a result of the increase in the applied load. Table 11 shows the specimen of the first crack load and the ultimate load that the specimen could bear. The development of linear cracks at the lower surface of the slabs is referred to as the crack resulting from the applied load, as shown in Fig. 8. The slab strengthened with polypropylene has the lowest bearing strength and was close to the reference slab because polypropylene fibers do not have high tensile strength like other fibers, as its maximum bearing strength was (45.3) kN, and the highest bearing strength among the specimens was the slab strengthen with carbon fiber mesh, which reached (56.6) ken, due to the high tensile strength possessed by carbon fibers. This indicates that it gave a significant improvement to the specimen by (29.0%) compared to the reference specimen. The specimens strengthened with polypropylene fibers and geogrid showed early initial cracking and were near to the initial cracking of the reference specimen and the improvement rate in them was (2.0%) for (PP) and (8.1%) for (GG) compared to the reference specimen. The specimens strengthened with fiberglass, carbon, and waste rubber meshes showed a significant improvement in terms of initial cracking by (15.9%), (26.9%) and (24.6%) respectively compared to the cpntrol slab.

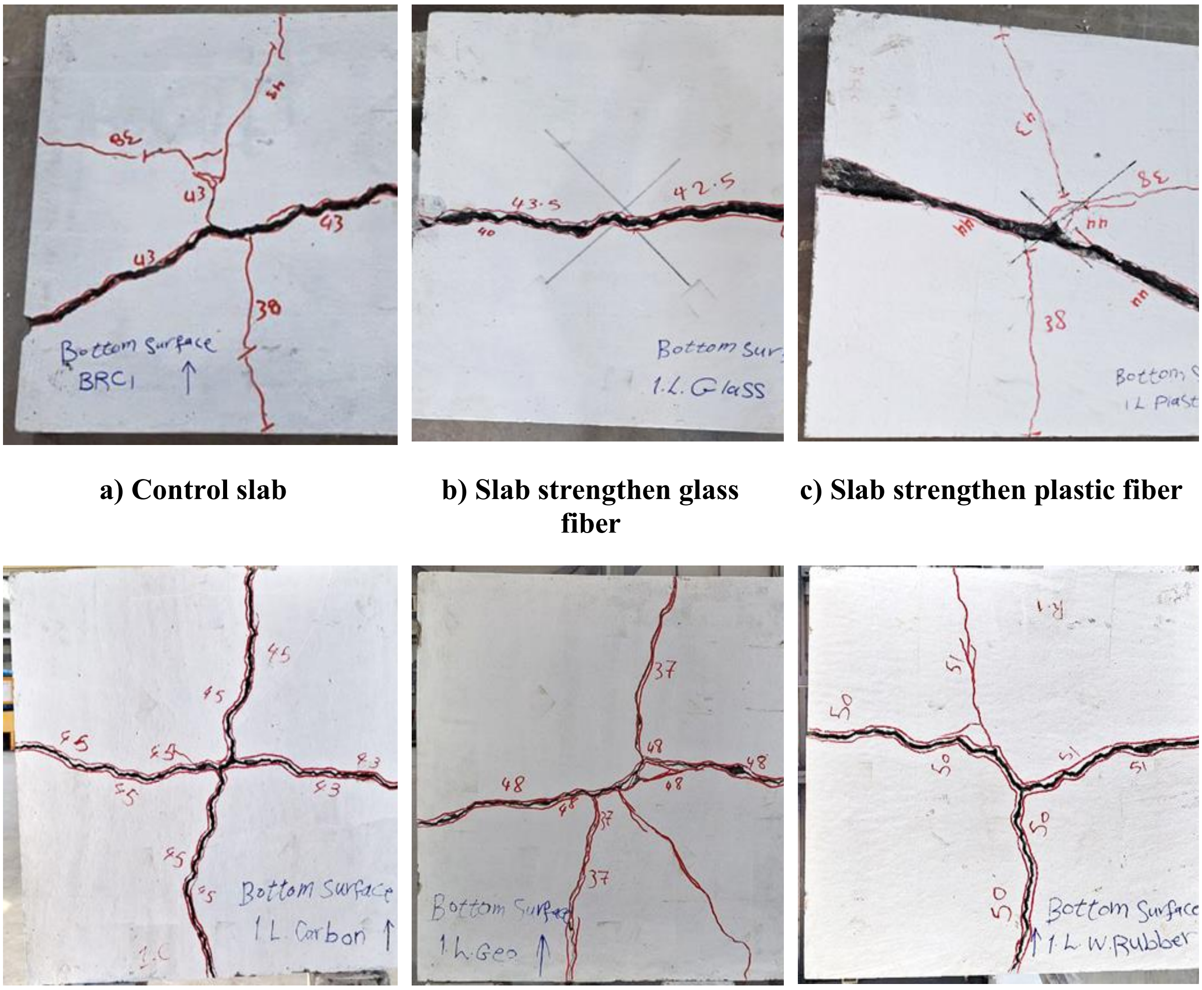

a) Control slab **b) Slab strengthen glass fiber** **c) Slab strengthen plastic fiber**

d) Slab strengthen carbon fiber **e) Slab strengthen geogrid fiber** **f) Slab strengthen waste rubber fiber**

Fig. 7: Concrete slab failure and crack patterns for center load

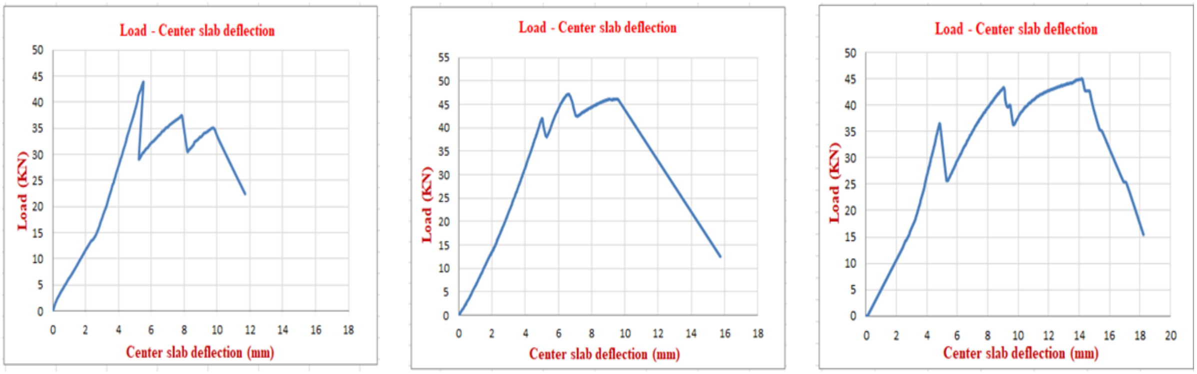

a) Control slab (BRC) b) (GL) C) (PP)

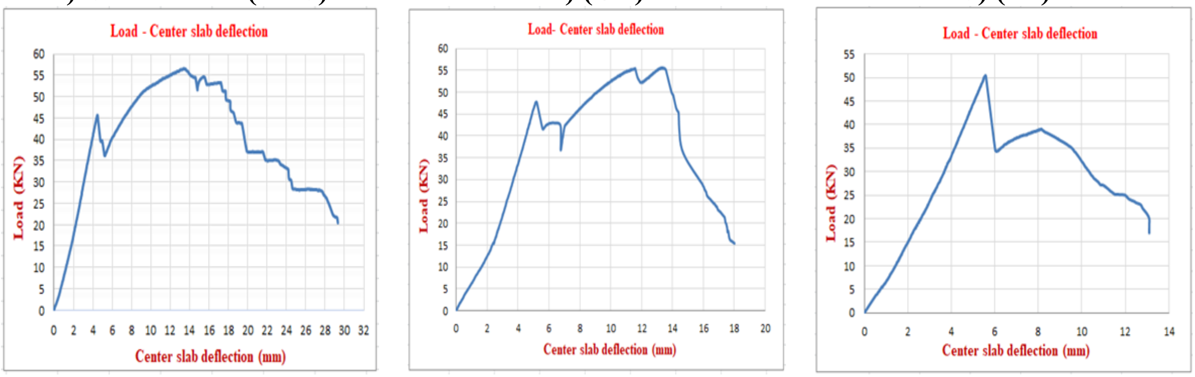

d) (CR) e) (GG) f) (WR)

Fig. (8): Mid-span deflection

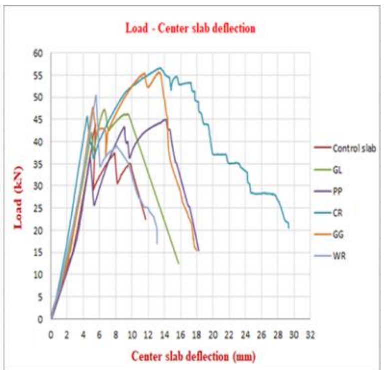

Fig. 9 Comparison of the behavior of slabs of concrete

3.4. Toughness

As shown in Table 11 and Fig. 10, the flexural toughness, also referred to as the total energy absorbed, was calculated by calculating the area under the load-deflection curve of the concrete slabs, where the toughness of the specimens strengthened with glass fiber mesh and polypropylene increased by (27.9%) and (49.8%) respectively compared to the reference specimen. The test specimens strengthened with carbon fiber mesh and geogrid showed a significant increase in toughness, which achieved an increase of (187%) for carbon and (77.4%) for geogrid compared to the reference slab. The results differed in the improvement of toughness when the toughness of the waste rubber strengthen specimen was calculated, as the improvement in it decreased by (12.9%) due to the low value of plasticity and deflection, despite the high load capacity of (15%) compared to the control slab.

Table 11: Load at first crack and ultimate failure with deflections of test specimens

Slab code	@ First crack		@ Ultimate		Toughness (kN.mm)	Increasing in Toughness %
	Load (kN)	Deflection (mm)	Load (kN)	Deflection (mm)		
BRC	34.6	4.64	43.9	5.52	371.45	——
GL	40.1	4.82	47.2	6.64	475.20	27.9
PP	35.3	4.72	45.3	14.2	556.37	49.8
CR	43.9	4.29	56.6	13.45	1066.06	187.0
GG	37.4	4.32	55.6	13.25	658.91	77.4
WR	43.1	5.35	50.4	5.58	419.45	12.9

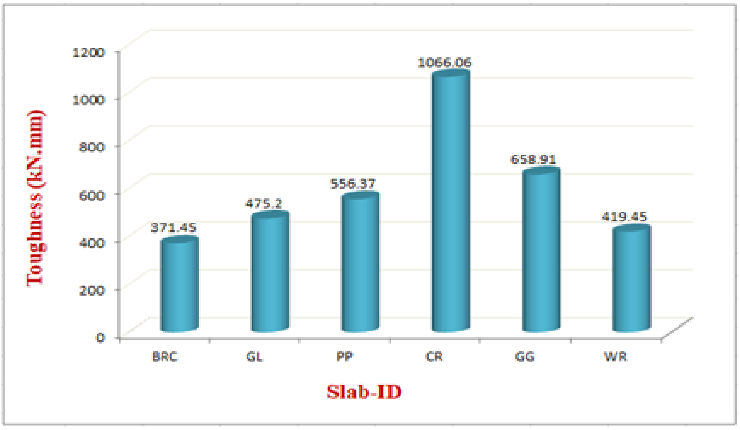

Fig. 10 Toughness of the tested slabs.

3.5. Ductility index and stiffness

Table 12 shows the yield load, the deflections in the center of the slab, and the ductility index for each slab. The ductility index is described as the ability of the structural element to withstand large deformations and is calculated by dividing the deflection at the failure point by the deflection at the initial yield. Through the results obtained, it was revealed that the specimen strengthened with carbon fiber mesh has a ductility value of (3.34), which is considered the highest value obtained through the experimental test. The ductility ratios of the slab strengthened with polypropylene fiber mesh were the lowest value obtained, which was (2.11). Table 13 shows the stiffness of the specimens and the percentage increase in the stiffness of the specimens strengthened with fiber mesh compared to the reference specimen, stiffness is calculated from the slope of the straight line at the beginning of the response curve (load-deflection curve) and at (20%) of the ultimate load value. Where the results indicated that the stiffness increased in the specimens strengthened with glass fiber, polypropylene, and waste rubber by (9.3, 8.1 and 12.8) %, respectively, compared to the reference specimen, While the stiffness increased significantly in the specimens strengthened with carbon fiber mesh and geogrid by the same percentage (33%) over the control specimen, this confirms the high stiffness that the concrete slab possessed from the fiber mesh.

Table 12: Load at yielding and Center deflection at (yield & failure) with ductility index

Slab code	Load at Yielding (kN)	Center deflection at yield (mm)	Center deflection at failure (mm)	Ductility index
BRC	42.3	5.34	11.70	2.19
GL	46.1	6.27	15.75	2.51
PP	42.1	8.64	18.24	2.11
CR	50.1	8.79	29.35	3.34
GG	50.2	9.00	18.00	2.00
WR	48.6	5.38	13.01	2.42

Table 13: Stiffness with increasing in stiffness in each specimen

Slabcode	Stiffness (kN/mm)	Increasing in stiffness (%)
BRC	8.6	———
GL	9.4	09.3
PP	9.3	08.1
CR	11.5	33.7
GG	11.4	32.6
WR	9.7	12.8

4. CONCLUSIONS

A number of experiments were conducted to examine the effects of various synthetic fiber mesh types on the stiffness; ductility index and toughness, of Winkler-foundation-based fiber strengthen concrete slabs. Based on this, the following conclusions have been made:

The mechanical properties, strength, deflection and crack width of concrete slabs strengthened with synthetic fiber meshes are positively affected. The test results show that in addition to improving the properties of concrete slabs, the presence of fiber meshes increases the strength of the slab to ultimate failure, and reduces its crack width. These improvements vary depending on the type of fiber mesh strength.

According to the test result, the use of fibers that act as a bridge for the cracks generated in the slab during testing significantly increases the strength of the concrete, as these fiber meshes increase the endurance of the slab, which in turn leads to raising the performance of the flexibility stage of the slab.

The growth cracks and increase in size will be reduced due to the presence of strengthened fiber meshes, especially in the slab strengthened with carbon fiber mesh, where the percentage of increase in the load for the appearance of the first crack reached 26.9% compared to the appearance of first cracks in the reference specimen not strengthen with fibers, and these fibers also improve the resistance of the section to tensile stresses and elastic deformations.

Fiber meshes improved the toughness of concrete slabs in general compared to the reference slab, as the highest percentage of increase was obtained in the specimen strengthened with carbon fiber mesh, at a rate of 187% compared to the reference specimen. This was due to the tensile strength of carbon fibers, which gave a noticeable and high increase to the specimen added to it, while the lowest increase was obtained in the specimen strengthened with rubber fiber mesh, which was at a rate of 12.9% compared to the reference specimen.

Based on the results obtained from the tests, a significant improvement in the stiffness of the specimens was observed, as the percentage of increase in the specimens strengthened with fiberglass mesh, polypropylene, and waste rubber was (9.3, 8.1 and 12.8) % respectively compared to the reference specimen, while in the other specimens the percentage of improvement was equal at (33.7) % compared to the reference specimen.

For the carbon fiber mesh strengthen slab, the highest percentage decrease was in the number of vertical cracks, their widths, and their extensions compared to the other slabs, which appeared with increasing loads and gradually enlarged. Followed by a small percentage of peripheral cracks. In addition, there was an increase in the failure load, which was (56.6) kN, compared to the failure load of the reference slab, which was (43.9) kN.

5. REFERENCES

Abbas, H.Q. and Al-Zuhairi, A.H. (2022) ‘Usage of EB-CFRP for Improved Flexural Capacity of Unbonded Post-Tensioned Concrete Members Exposed to Partially Damaged Strands’, Civil Engineering Journal (Iran), 8(6), pp. 1288–1303. Available at: https://doi.org/10.28991/CEJ-2022-08-06-014.

ACI (2006) ‘ACI 360R-06 Design of Slabs on Ground’, Aci 360R-06, pp. 1–72.

Aljebory, S.M. and Kamonna, H.H. (2025) ‘Repairing of Continuous One-Way Reinforced Concrete Slabs By Cfrp Composites’, Kufa Journal of Engineering, 16(1), pp. 324–343. Available at: https://doi.org/10.30572/2018/KJE/160119.

Baarimah, A.O. and Syed Mohsin, S.M. (2017) ‘Behaviour of reinforced concrete slabs with steel fibers’, IOP Conference Series: Materials Science and Engineering, 271(1). Available at: https://doi.org/10.1088/1757-899X/271/1/012099.

Etefa, G. and Mosisa, A. (2020) ‘Waste Rubber Tires: A Partial Replacement for Coarse Aggregate in Concrete Floor Tile Production’, American Journal of Civil Engineering, 8(3), p. 57. Available at: https://doi.org/10.11648/j.ajce.20200803.12.

Ischenko, A. and Borisova, A. (2020) 'Application of fiber-reinforced concrete in high- rise construction', 02005.

Jaber, A.A., Mohammed, A.S. and Abbas, S.A. (2021) 'Behavior and strength of polypropylene reinforced concrete slabs', Journal of Engineering Science and Technology, 16(2), pp. 1746–1760.

Journal, K. (2010) 'Notation : 2 . Test program ':, 1(2), pp. 62–71.

Kamonna, H.H. and Al-sada, D.J.A. (2021) 'EFFECT OF NEAR-SURFACE MOUNTED BARS ON THE STRUCTURAL BEHAVIOR OF ONE-WAY RC SLAB', 12(3), pp. 12–30.

Koerner, R.M. (2005) 'Designing with geosynthetics- 2Th Edition', p. 652.

Milind V. Mohod (2015) 'Performance of Polypropylene Fibre Reinforced Concrete\n', IOSR Journal of Mechanical and Civil Engineering (IOSR-JMCE), 12(1), pp. 28–36. Available at: https://doi.org/10.9790/1684-12112836.

Nimnim, H.T. and Fakhri, A.H. (2022) 'STRUCTURAL BEHAVIOR OF HIGH STRENGTH ARCHED', 13(2), pp. 1–15.

Roesler et al (2006) 'ACI-Synthetic-2006', Effect of Synthetic Fibers on Structural Behavior of Concrete Slabs-on-Ground, M01(103), pp. 3–10.

Shi, F. et al. (2023) 'Comparative performance analysis of ground slabs and beams reinforced with macro polypropylene fibre, steel fibre, and steel mesh', Structures, 56(July), p. 104920. Available at: https://doi.org/10.1016/j.istruc.2023.104920.

Sorelli, L.G., Meda, A. and Plizzari, G.A. (2006) 'Steel fiber concrete slabs on ground: A structural matter', ACI Structural Journal, 103(4), pp. 551–558. Available at: https://doi.org/10.14359/16431.

Sucharda, O. et al. (2017) 'Comparative evaluation of mechanical properties of fibre-reinforced concrete and approach to modelling of bearing capacity ground slab', Periodica Polytechnica Civil Engineering, 61(4), pp. 972–986. Available at: https://doi.org/10.3311/PPci.10688.

Suksawang, N., Mirmiran, A. and Yohannes, D. (2014) 'Use of Fiber Reinforced Concrete for Concrete Pavement Slab Replacement (Florida Department of Transportation Research Report BDK80 TWO 977-27)', (March), pp. 26–27.

Tahwia, A.M. et al. (2024) ‘Experimental investigation of rubberized concrete slab-on-grade containing tire-recycled steel fibers’, Innovative Infrastructure Solutions, 9(2), pp. 1–16. Available at: https://doi.org/10.1007/s41062-023-01354-9.